JOURNAL OF VIROLOGY, Dec. 2011, p. 12474–12481 Vol. 85, No. 23
0022-538X/11/$12.00 doi:10.1128/JVI.05344-11

Hepatocytes Traffic and Export Hepatitis B Virus Basolaterally by Polarity-Dependent Mechanisms▽

Purnima Bhat,[1,2,3]* Michelle J. Snooks,[1] and David A. Anderson[1,3,4]

Ian Potter Hepatitis Research Laboratory, Macfarlane Burnet Institute for Medical Research and Public Health, 85 Commercial Rd., Melbourne 3004, Australia[1]; Diamantina Institute, The University of Queensland, Woolloongabba 4102, Australia[2]; Department of Microbiology and Immunology, University of Melbourne, Melbourne, Australia[3]; and Department of Microbiology and Department of Immunology, Monash University, Melbourne, Australia[4]

Received 12 June 2011/Accepted 12 September 2011

Viruses commonly utilize the cellular trafficking machinery of polarized cells to effect viral export. Hepatocytes are polarized *in vivo*, but most *in vitro* hepatocyte models are either nonpolarized or have morphology unsuitable for the study of viral export. Here, we investigate the mechanisms of trafficking and export for the hepadnaviruses hepatitis B virus (HBV) and duck hepatitis B virus (DHBV) in polarized hepatocyte-derived cell lines and primary duck hepatocytes. DHBV export, but not replication, was dependent on the development of hepatocyte polarity, with export significantly abrogated over time as primary hepatocytes lost polarity. Using Transwell cultures of polarized N6 cells and adenovirus-based transduction, we observed that export of both HBV and DHBV was vectorially regulated and predominantly basolateral. Monitoring of polarized N6 cells and nonpolarized C11 cells during persistent, long-term DHBV infection demonstrated that newly synthesized sphingolipid and virus displayed significant colocalization and fluorescence resonance energy transfer, implying cotransportation from the Golgi complex to the plasma membrane. Notably, 15% of virus was released apically from polarized cells, corresponding to secretion into the bile duct *in vivo*, also in association with sphingolipids. We conclude that DHBV and, probably, HBV are reliant upon hepatocyte polarity to be efficiently exported and this export is in association with sphingolipid structures, possibly lipid rafts. This study provides novel insights regarding the mechanisms of hepadnavirus trafficking in hepatocytes, with potential relevance to pathogenesis and immune tolerance.

Hepatocytes are polarized epithelial cells with distinct apical and basolateral domains facing the bile canaliculi and the hepatic sinusoid, respectively. Tight junctions between cells form a barrier between blood and bile. Direct apical transport of synthesized proteins from the *trans*-Golgi network (TGN) plays a minor role in hepatocytes and similarly in hepatocyte-derived HepG2 cells (16, 39). Instead, proteins destined for the apical membrane are usually transported to the basolateral membrane and sorted in basolateral early endosomes, before transport to the apical surface (21, 41). Sphingolipid sorting in epithelial cells results in both apical and basolateral transport by differentially regulated mechanisms (42).

The role of epithelial cell polarity in viral entry and export has been extensively investigated for a broad number of pathogens, using cell culture models of columnar epithelia. These studies point to cell-specific, virus-specific transportation mechanisms that have a significant relationship with clinical pathophysiology. Epstein-Barr virus, for example, is exported nonvectorially in mucosal epithelial cells (30), correlating with its local and systemic infection, while rotavirus infects intestinal cells apically and is released via the same domain into the gastrointestinal lumen, largely limiting its serious clinical effects to the gastrointestinal tract (9). Recently, we showed that hepatitis A virus (HAV) was exported from the basolateral domain of polarized hepatocytes (26), contrary to the expected biliary export of the virus and in contrast to what was seen previously in similar studies using enterocyte-derived cells (3), demonstrating the importance of using relevant hepatocyte-derived cell lines to study interactions for hepatotropic viruses.

Persistent hepatitis B virus (HBV) infection causes liver cirrhosis and hepatocellular carcinoma. Hepadnaviruses, including both HBV and duck hepatitis B virus (DHBV), share many aspects of their replication and infectivity behavior: they reproduce exclusively in hepatocytes, are assembled in the Golgi complex, and are exported to reenter the bloodstream. It is therefore probable that the virus is exported predominantly via the basolateral domain for release into the viral sinusoid, as markers of viral replication in hepatocytes correlate with viremia. Localization of DHBV at the basolateral surface of duck hepatocytes also suggests that the virus is exported from this plasma membrane (6). It has also been suggested that HBV budding is reliant on the host endosomal sorting complex required for transport (ESCRT) machinery, which regulates trafficking of cargo into vesicular bodies for transportation through the cell (12), although this was in a nonhepatocyte, nonhuman cell line and in a cell transfection and not infection system. The mechanism by which hepatocytes transport hepadnaviruses and whether they vectorially sort viruses before export are unknown.

HBV establishes persistent infection in hepatocytes, driven from a nuclear pool of covalently closed circular DNA. Cultured cell lines are generally refractory to HBV infection, but

* Corresponding author. Mailing address: Diamantina Institute, University of Queensland, Ipswich Road, Queensland, Woolloongabba 4102, Australia. Phone: 61 7 3240 5944. Fax: 61 7 3240 5946. E-mail: purnima@uq.edu.au.

▽ Published ahead of print on 21 September 2011.

replication can be established in hepatocyte-derived lines via transient or stable transfection or transduction with vectors. High viral replication levels have been achieved with recent models using novel dual-transfection systems (14). These models have revealed many details of hepadnavirus replication, assembly, and release, but most hepatocyte-derived cell lines are nonpolarized. Previously, we have developed an HepG2-derived cell line (N6) that retains characteristic features of polarized hepatocytes but displays the morphology of simple columnar epithelia, allowing conventional studies of virus trafficking and release (26). Here we have used N6 cells transfected or transduced with HBV or DHBV to reveal the first details of hepadnavirus trafficking and export in relevant polarized cells. Current hepatocyte culture models cannot be infected with hepatitis B virus. We have therefore used DHBV as a representative hepadnavirus in many of the experiments described here, allowing us to examine the export of infectious virions from physiologically relevant, polarized hepatocyte-derived cell lines by subsequent titration of infectious virus on primary duck hepatocytes (PDHs) in culture.

MATERIALS AND METHODS

Materials. Brefeldin A and human albumin were from Sigma-Aldrich: goat anti-rabbit Alexa 488, goat anti-mouse Alexa 586, Alexa 568 holotransferrin, BODIPY-TR-C_5 ceramide complexed to bovine serum albumin, and TOTO-3 were from Molecular Probes. PCR was performed using iQ SYBR green Supermix (Bio-Rad) in a Bio-Rad iQ LightCycler apparatus and primers supplied by Geneworks (Australia).

Cell lines. HepG2 subclones N6 and C11 (26) were maintained in minimal essential medium with 1% penicillin and streptomycin, 1% glutamine, and 10% fetal bovine serum. Cells were seeded onto (0.4-μm-pore-size) 25-mm Transwell collagen-coated inserts (Costar) and used 14 days later. N6 and C11 cells were also used to establish the DHBV-infected cell lines DVP and DVNP, respectively, using a strategy of transient transfection and short-term drug treatment to eliminate nontransfected cells without necessarily selecting for stable transfection. A linear 1.3 genome length of DHBV was amplified from pUC119-DHBV (kind gift from Ulla Protzer) using primers flanking the full 1.3-length viral genome and ligated into pCI-Neo (New England BioLabs) before transformation in *Escherichia coli*. The resultant plasmid, pCI-Neo.DHBV, was transfected into N6 and C11 cells using Lipofectamine (Invitrogen), and cells were treated with 800 μg/ml G418 for 10 days. Microcolonies of cells were trypsinized using cloning cylinders and seeded into 96-well plates in G418-containing medium for 48 h, representing about five population doubling times with drug selection. Cells were subsequently maintained and passaged every 14 days without G418 selection, and clones DVP and DVNP that maintained the morphology of N6 or C11 cells and exhibited persistent production of DHBV were selected.

Vectors and transduction. Defective adenovirus vectors allow the efficient transduction of HepG2 cells with transient production of infectious DHBV or HBV (27). Adenovirus vector containing green fluorescent protein (GFP) and the DHBV genome (adeno-GFP-DHBV) and adeno-GFP-HBV were kindly provided by Ulla Protzer (Germany) and Joe Torresi (Australia), respectively. Transwell membrane-cultured N6 and C11 cells were transduced with 10^6 infectious particles of adeno-GFP-HBV or adeno-GFP-DHBV via the basolateral domain. Transwells were washed, and cells were incubated at 37°C until GFP expression was first detectable by immunofluorescence microscopy.

Primary duck hepatocytes. Animal experimentation was approved by the Alfred Medical Research and Education Precinct Animal Ethics Committee. DHBV-positive PDHs were obtained by infecting day-old Pekin-Aylesbury ducklings with DHBV (strain D16). Seven days later, duckling livers were collagenase perfused as previously described (31). PDHs were maintained in Williams E medium with 10 mM Tris, pH 7.6, 6 mM HEPES, 0.02% sodium bicarbonate, 1% penicillin, 1% streptomycin, 1% glutamine, 0.02% glucose, 10 μM hydrocortisone 21-hemisuccinate, 0.01% insulin, and 1.5% dimethyl sulfoxide. Supernatants from adeno-GFP-DHBV-transduced or persistently infected cell lines were applied to DHBV-negative PDHs in serial dilutions (1) to determine the infectious virus titer. Cells were checked for GFP expression after 3 days to confirm the absence of carryover adeno-GFP-DHBV particles. Coverslips were fixed after 7 days. DHBV-positive foci were quantified by indirect immunofluorescence.

Quantitative PCR. Quantitative PCRs were performed using primers DHBV 03 (ACTAGAAAACCTCGTGGACT) and DHBV 04 (GGGAGAGGGGAGC CCGCACG) or HBV PC1 (GGGAGGAGATTAGGTTAA) and HBV PC2 (GGCAAAAACGAGAGTAACTC) (15, 37).

Southern blotting. Briefly, cells were lysed by freeze-thaw 3 times in phosphate-buffered saline (PBS). Nuclei were pelleted out. Samples were treated with DNase I to remove nonencapsidated chromosomal DNA. Proteinase K was used to degrade capsid proteins and release viral DNA. Samples were sequentially phenol and chloroform extracted, and viral DNA was ethanol precipitated overnight. Samples were RNase treated and electrophoresed on a 1% agarose gel. The gel was washed in 0.25 M HCl and then sequentially washed in buffers (1.5 M $CaCl_2$, 0.5 M NaOH, followed by 1.5 M NaCl, 0.25 M NaOH). The DNA was transferred to a positively charged nylon membrane by capillary transfer overnight in SSC (1× SSC is 0.15 M NaCl plus 0.015 M sodium citrate). The membrane was baked at 120°C for 20 min and hybridized with a full-length [^{32}P]dCTP-labeled DNA probe (Perkin Elmer, Australia) using a random priming kit (Amersham). Hybridized blots were exposed to Hyperfilm-ER (Amersham).

Western blotting. Intracellular protein analysis was performed for the detection of L and S proteins, which reside in the endoplasmic reticular membranes of the cell. Cell lysate was fractionated to isolate the membrane fraction. Samples were electrophoresed through a 13% SDS-polyacrylamide gel in a Mini-Protean II apparatus (Bio-Rad). Proteins were transferred onto a Hybond-C nitrocellulose membrane (Amersham) using a Trans-Blot semidry transfer cell (Bio-Rad). Membranes were blocked in 3% skim milk powder in PBS, followed by probing using mouse anti-DHBV pre-S primary antibody (1H1) in 1% skim milk powder in PBS–Tween 20 for 60 min. Alexa 680 anti-mouse secondary antibody was added, and membranes were visualized on an Odyssey fluorescence plate reader (Li-Cor Biosciences).

Indirect immunofluorescence. Fixed cells were treated with 1H1 antibody and rabbit anti-ZO-1 antibody and counterstained with Alexa 568 goat anti-mouse and Alexa 488 goat anti-rabbit secondary antibodies; nuclei were stained with TOTO-3.

Transferrin studies. DHBV-infected monolayers of PDHs and DVP and DVNP cells were pulsed with 0.05 mg/ml Alexa 568-labeled transferrin at 4°C for 15 min and then warmed to 37°C for 2 h. Cells were then washed and cooled rapidly to 18°C for 60 min to hold all endosomal and Golgi complex-related traffic (32). Brefeldin A (1 μg/ml) or vehicle (equivalent units ethanol) as a no-drug control was added, and cells were further incubated at 18°C for 15 min. Coverslips were collected at time zero, and the cells were warmed to 37°C. Coverslips were collected and fixed in 4% paraformaldehyde with 1% Triton X-100 for immunofluorescence.

Sphingomyelin studies. PDHs (DHBV infected) were cultured on coverslips, incubated with 5 μM BODIPY-TR-C_5 ceramide for 30 min at 4°C, and rinsed in ice-cold medium before incubation at 18°C for a further 30 min to hold all newly manufactured sphingolipids at the Golgi complex. Five percent bovine serum albumin (BSA) was added to the cells to capture any basolaterally appearing sphingolipid. Brefeldin A at 1 μg/ml or vehicle was added, and cells were further incubated at 18°C for 15 min. Cells were then warmed rapidly to 37°C to release Golgi complex traffic, coverslips were collected at 0 and 30 min and fixed with paraformaldehyde, and viral antigen was visualized with 1H1 and Alexa 488 goat anti-mouse antibodies.

Microscopy. We used a Zeiss LSM 510 META microscope with a ×60 oil-immersion objective lens. Fluorescence resonance energy transfer (FRET) images between Alexa 488 and Alexa 568 were obtained by excitation at 488 nm with an HFT 488-nm dichroic mirror and an LP 560-nm emission filter. In this pair, 488-nm-stimulated molecules (donor) emit sufficient light to excite a molecule at 568 nm (acceptor), which will in turn emit light in the 568-nm+ spectrum. To ensure that we minimized any bleed-through effect, we analyzed images in the 610-nm emission spectrum. Additionally, single-stained control images were taken to confirm minimal bleed through. Raw images were analyzed with the ImageJ program. Images were processed with Adobe Photoshop software.

Statistical analysis. Mean values with standard errors of the means are given. Significance of differences was determined by unpaired two-tailed Student's *t* test. We accepted values of P of <0.05 to be significant.

RESULTS

Virus export is both dependent on cell polarity and vectorial. We have observed that a significant proportion of primary

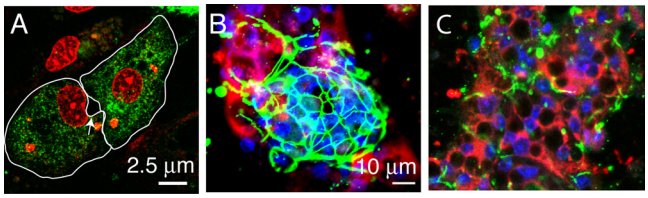

FIG. 1. DHBV export is dependent on cell polarity in primary hepatocytes. Primary duck hepatocytes were prepared from a duckling congenitally infected with DHBV and cultured for 6 days. (A) A polarized couplet of hepatocytes in culture forms apical surfaces with tight junctions, resembling a bile ductule (arrow). Green, DHBV; red, nuclei. (B and C) Colonies may be polarized (B), showing differential intracellular viral staining (red) between central polarized cells (ZO-1, green) and peripheral nonpolarized cells, suggesting preferential viral export from polarized cells. In contrast, nonpolarized colonies (C) show no ZO-1 staining and marked intracellular virus accumulation.

duck hepatocytes (PDHs) will reestablish polarity for a variable time in culture following preparation by collagenase perfusion. We examined the distribution of virus and ZO-1 as a marker of cell polarity in clusters of congenitally DHBV-infected PDHs in culture. Figure 1A shows a primary hepatocyte couplet in culture demonstrating the formation of the apical surface (bile ductule) and tight junction contact points between cells. Figure 1B shows a hepatocyte cell cluster with evidence of early development of polarity in the center, demonstrated by extensive tight junction formation (ZO-1), while peripheral cells have not established polarity due to a lack of cell contacts at the edge. Congenital DHBV infection leads to ubiquitous infection throughout the liver, but the nonpolarized peripheral cells show considerably more staining for virus-specific antigen than the central, polarized cells. In contrast, Fig. 1C shows a cluster of infected PDHs without evidence of cell polarity and DHBV staining in all cells, suggesting that the position in the cluster and intercellular contacts *per se* do not inhibit viral replication. From these observations, we postulated that polarized hepatocytes may export virus efficiently, while nonpolarized cells retain virus.

We investigated the kinetic relationship between cell polarity and export of infectious virus from DHBV-infected PDHs over 30 days in culture (Fig. 2). Intracellular virus was present at high levels on days 1 to 6, but exported virus was not detected until day 9 (Fig. 2A). From days 12 to 18, the level of virus export increased dramatically, accompanied by a decline in intracellular virus. This period coincides with development of polarity in the PDH culture, demonstrated by extensive tight junction formation (Fig. 2B). At 18 days, the total amount of infectious virus recovered from the culture was somewhat reduced, but the large majority of this was still exported from the cells, which remained polarized, as demonstrated by ongoing vectorial export of albumin. From 24 days, polarity was progressively lost, with a coincident decline in viral export and a proportional increase in intracellular virus and with high yields of infectious virus almost exclusively retained within the cells at 30 days. These data strongly suggested that in primary infected hepatocytes, establishment and maintenance of cell polarity were associated with efficient export of DHBV.

PDHs do not establish continuous cell monolayers in Transwell inserts. In contrast, N6 cells can be successfully grown in

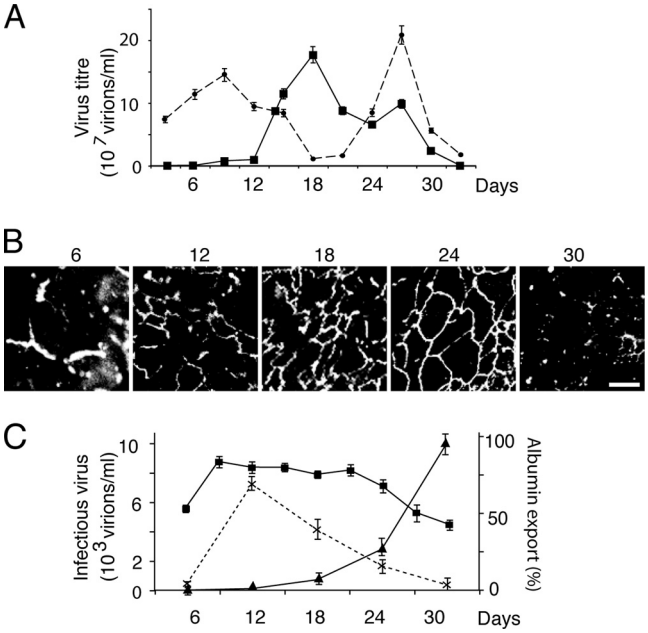

FIG. 2. Kinetics of infectious viral export. (A) Congenitally infected PDHs were cultured for 30 days. Viral export (squares) significantly increased after day 12 as intracellular virus levels (circles) fell. After day 27, virus was retained intracellularly as export fell. (B) Viral secretion correlates with formation of tight junctions (ZO-1) and their subsequent loss (day 30). (C) In adeno-DHBV-transduced polarized N6 cells, declining functional polarity determined by vectorial albumin transport (squares) was associated with a significant reduction in viral export (crosses) and a corresponding increase in intracellular virus accumulation (triangles).

this manner, and the vectorial export of albumin at their basolateral domain provides a functional measurement of cell polarity (26). N6 cells were transduced with adeno-GFP-DHBV at 6 days after seeding, and supernatant and cell lysates were examined for infectious virus over 30 days postransduction (Fig. 2C). By day 12 (6 days postransduction), cells were highly polarized and also showed high levels of viral export, with minimal accumulation of intracellular virus. The degree of cell polarity and virus export declined thereafter, with progeny virus almost exclusively retained within the cells by day 30, supporting the strong relationship between cell polarity and the efficiency of DHBV export seen in PDHs.

We then examined vectorial release of virus from polarized and nonpolarized cells transduced with adeno-GFP-DHBV or with adeno-GFP-HBV. Polarized N6 cells exported more than 75% of progeny HBV (measured by real-time PCR) and infectious DHBV into the basolateral domain, whereas equal proportions were exported from nonpolarized cells to the apical and basolateral compartments of the Transwell apparatus (Fig. 3A).

Hepatocyte export pathways. We disrupted intracellular hepatocyte transport routes to map viral export pathways in hepatocytes. Infected primary hepatocytes were treated with brefeldin A, and replicate 6-h collections of supernatant were collected before and after drug treatment and analyzed by real-time PCR. Brefeldin A treatment of infected PDHs resulted in a marked (≈2.5-fold) reduction of total virus export,

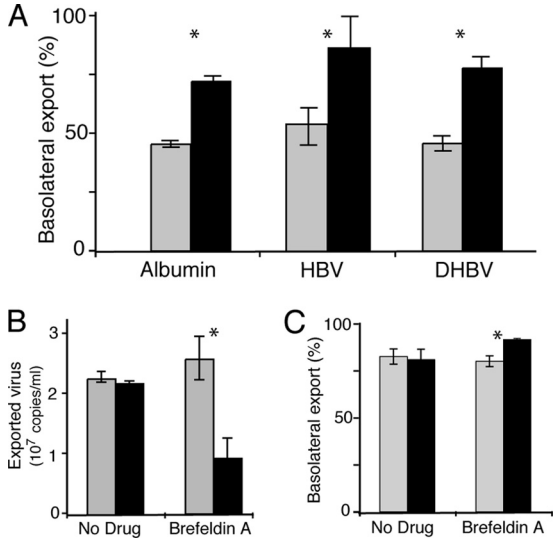

FIG. 3. Viral traffic in hepatocytes. (A) N6 cells (black) grown on membranes and transduced with adeno-GFP-HBV or adeno-GFP-DHBV demonstrate vectorial export of both albumin and virus predominantly to the basolateral domain, while C11 cells (gray) show nonvectorial secretion. Nonpolarized cells secreted albumin and virus nonvectorially. (B) Viral traffic is dependent on the TGN and endosomal system. Treatment (black) with brefeldin A to disrupt the vesicular transport system results in a marked reduction in total virus export from PDHs (pretreatment, gray), whereas export is maintained at constant levels during mock treatment (No Drug). *, $P < 0.05$. (C) Apical transportation of virus from the Golgi complex. Brefeldin A treatment resulted in an increase in viral export to the basolateral domain, implying a preferential inhibition of apical transportation with brefeldin A.

suggesting that active Golgi complex and endosomal viral transport are required for efficient hepadnaviral release from primary liver cells (Fig. 3B).

We noted above (Fig. 3A) that while the majority of virus export from polarized HepG2 cells was basolateral, a small proportion of the virus (about 12%) was released at the apical domain. Interestingly, when we applied brefeldin A to polarized HepG2 N6 Transwell cultures that had been transduced with adeno-HBV (multiplicity of infection, 1), there was a significant increase in the proportion of virus exported to the basolateral domain, from 78% to over 90% ($P = 0.023$) (Fig. 3C). As brefeldin A disrupts the Golgi complex and inhibits TGN-related sorting (5, 35), these data suggest that while most substrates are preferentially transported by Golgi complex-dependent and Golgi complex-independent means to the basolateral surface in hepatocytes (Fig. 3C), active sorting via a brefeldin A-sensitive pathway directs some virus to the apical surface.

Development of persistently infected cells. In order to more closely model viral trafficking within polarized hepatocytes persistently infected with hepadnaviruses, we developed DVP and DVNP cells, which are polarized N6 and nonpolarized C11 cells, respectively, persistently infected with DHBV but without the adenoviral vector, which interferes with cell integrity over the course of longer experiments. In these DVP and DVNP cells, DHBV production was established by transient transfection and short-term G418 treatment to eliminate non-transfected cells, but without long-term drug treatment to select stably transfected cells. Both cell lines secreted high titers of DHBV, peaking at over 5×10^8 copies/ml/day from DVP and over 2×10^8 copies/ml/day from DVNP, detected using real-time PCR, with 10-fold lower titers of infectious virus being detected by infection of PDHs. These lines retained the polarity of the parent cells, with DVP cells showing apical ZO-1 staining in a honeycomb pattern (Fig. 4A), vectorial albumin export to the basolateral domain, and virus export basolaterally (Fig. 4B), while the DVNP cells showed no organized ZO-1 staining and exported albumin equally to both apical and basolateral Transwell compartments. DVP cell lysate contained double-stranded and single-stranded DHBV DNA (Fig. 4C). Western blot of lysates shows production of viral L and S proteins (Fig. 4D), confirming that intracellular viral replication of DHBV is occurring through viral replicative intermediates and via viral protein production.

Virus traffic is independent of transcytosis. Hepatocytes manufacture vast quantities of substrates which are exported from the cell, predominantly into the sinusoid via the basolateral domain. Synthesized protein is transported directly to the basolateral domain, with any apically directed molecules then subsequently transcytosing to the apical membrane (23). Like other epithelial cells, they also transcytose extracellular proteins. Unique among epithelial cells, hepatocytes both transcytose transferrin from the extracellular environment and synthesize it *de novo*. The bulk of the transcytosed transferrin returns to the basolateral plasma membrane, but a small, slow pathway has been shown to take some of it to the apical surface in HepG2 cells (38). The well-defined transferrin transcytosis pathway intersects with its biosynthetic pathway at the TGN (4, 28). PDHs and DVP cells (both of which are polarized) and DVNP cells (nonpolarized) were pulsed with Alexa 568-labeled transferrin and examined by confocal microscopy. At 37°C, colocalization of transferrin and DHBV was significantly higher in nonpolarized cells than polarized cells (Fig. 5). Inhibition of transport from the Golgi complex with brefeldin A resulted in perinuclear Golgi complex localization of both virus and transferrin (Fig. 5A, parts B, D, and F). These data imply that transferrin and DHBV share only a part of the transportation pathways in the hepatocyte and that this differential transportation is polarity dependent.

Hepatocytes export DHBV with sphingomyelin. Sphingomyelin and glucosylceramide are synthesized from ceramide in the Golgi complex. Sphingomyelin is transported to the basolateral cell surface, while glucosylceramide is transported first to the apical surface before transcytosis (22). These sphingolipids are associated with rafts and trafficking in polarized cells, including hepatocytes (8, 21, 25). As we had observed that a proportion of DHBV was directly released at the apical domain (Fig. 3A and C), the association of sphingolipids with viral transport was investigated.

In the Golgi complex of HepG2 cells, labeled ceramide forms labeled sphingomyelin and glucosylceramide, which are vectorially transported to the plasma membrane (21, 32–34, 42). Infected PDHs were pulsed with labeled ceramide and stained for virus as described above, with BSA added to the medium to capture exported sphingolipids and prevent recycling. There was marked colocalization of sphingolipid and viral envelope antigen in primary hepatocytes (Fig. 6A). Virus

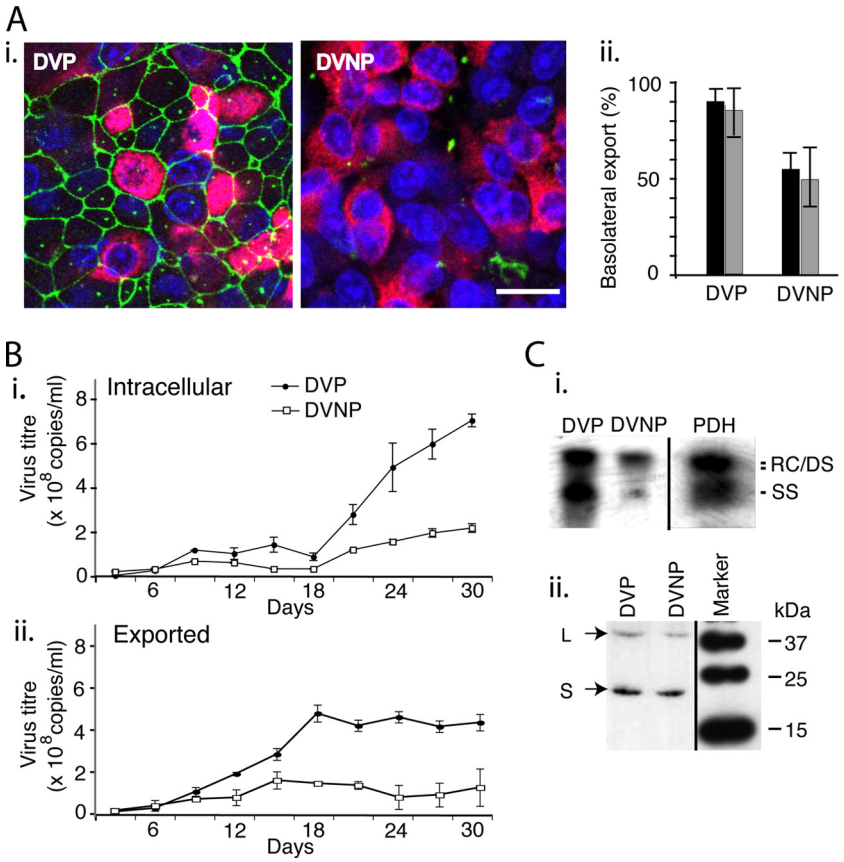

FIG. 4. Cell lines persistently infected with DHBV. (A) (i) DVP and DVNP cells express DHBV surface antigen (red), but the ZO-1 (green) distribution indicates that only DVP cells are polarized. Bar, 5 μm. (ii) When grown on membranes, DVP cells export a much greater percentage (almost 100%) of the total virus (black bars) produced basolaterally than the nonpolarized DVNP cells, which parallels polarized albumin secretion (gray bars). (B) These cell lines export virus efficiently (ii) with low intracellular levels (i) until 24 days of culture. (C) (i) Southern blotting of lysates shows that the cell lines produce all intracellular DHBV viral replicative DNA intermediates: relaxed circular (RC), double-stranded (DS), and single-stranded (SS) DNA. (ii) Western blotting shows both L and S antigens in lysates.

and sphingolipid remained colocalized at the Golgi complex in the presence of brefeldin A, suggesting cotransportation and shared mechanisms of sorting and trafficking.

We further investigated the colocalization of sphingolipid and hepadnavirus by analyzing FRET between these molecules in primary hepatocytes. Figure 6B shows high-signal FRET between labeled sphingolipid and virus in primary hepatocytes. DVP and DVNP cells pulsed with BODIPY-TR-C_5 ceramide showed synthesized sphingolipid and DHBV colocalized and demonstrated a FRET signal regardless of cell polarity. Photobleaching of acceptor molecules showed marked donor fluorescence recovery, confirming FRET interaction between DHBV and sphingolipid (Fig. 7). These data strongly suggest that progeny hepadnaviruses and endogenous sphingolipid are cotrafficked in hepatocytes, resulting in predominant basolateral release but with significant levels of direct apical release.

DISCUSSION

Hepatocyte polarity is intrinsic to the synthetic and metabolic functions of the liver. The formation of plasma membrane polarity is influenced by the asymmetric distribution of post-Golgi complex transport proteins, implicating a fundamental relationship between Golgi complex transport and membrane polarity formation (10, 36). Studies of HAV in the N6 cell line revealed unexpected basolateral export of this enterically transmitted virus (26), underscoring the importance of using polarized hepatocyte-derived cells to study trafficking of hepatotropic viruses. Conversely, HBsAg has been used as a protein to model cell-specific mechanisms of vectorial sorting (18), but the apical sorting of HBsAg observed in MDCK (canine kidney) cells is unlikely to be relevant to HBV replication in the liver since massive quantities of HBsAg are found in the plasma, reflecting predominant basolateral sorting in hepatocytes, as we have observed here and previously with HAV (26).

Hepatitis B virus, along with other hepadnaviruses, is noncytopathic and strictly hepatotropic. The small viral genome requires that it utilize cellular machinery for many of its functions, a factor that contributes to its exclusive hepatotropism. It is known that viral envelope proteins are assembled and modified in the endoplasmic reticulum (ER) and associate with the genome-containing core on passage through the ER-Golgi complex before export (13). Additionally, HBV export pathways that involve regulated endosomal structures and even some that are independent of the endosomal machinery have

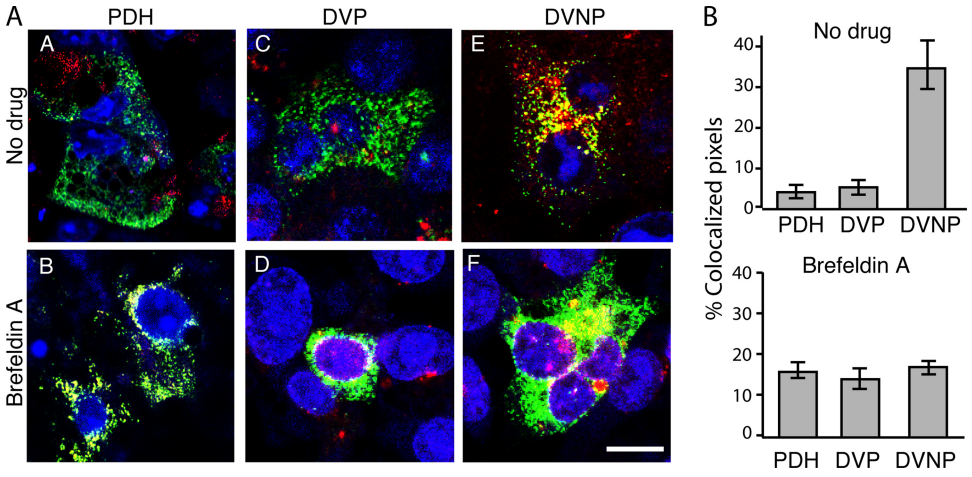

FIG. 5. Virus traffics with transferrin in polarized hepatocytes. (A) DHBV-infected polarized PDHs (parts A and B) and DVP cells (parts C and D) and nonpolarized DVNP cells (parts E and F) were exposed to exogenous transferrin (red). There is minimal colocalization of transferrin and virus throughout the cytoplasm in both hepatocytes and DVP cells (parts A and C) compared to nonpolarized cells (part E). Brefeldin A treatment resulted in Golgi complex localization of transferrin and virus, regardless of polarity (parts B, D, and E). Bar, 5 μm. (B) Colocalization was quantified over each field in treated and untreated cells. Averages of at least nine fields over 3 experiments are given.

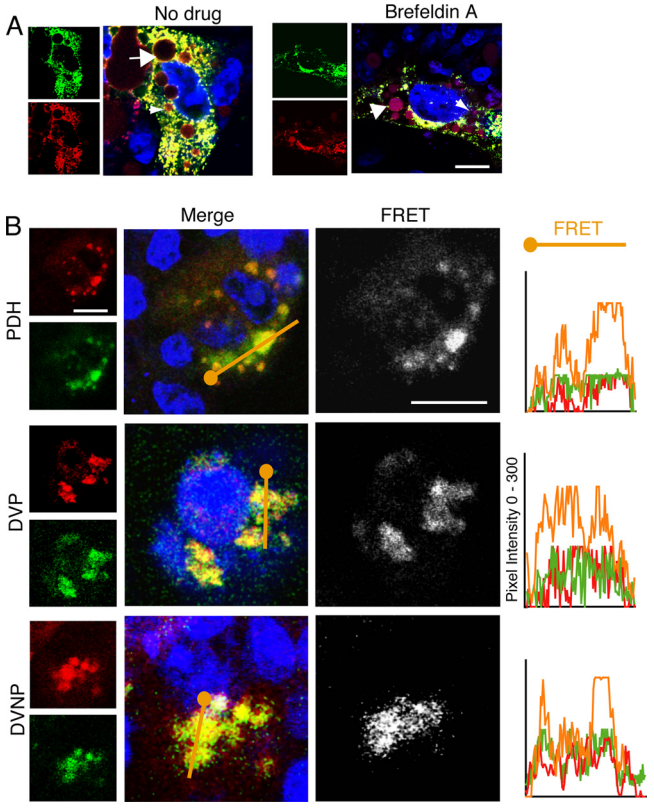

FIG. 6. DHBV colocalizes with sphingolipid. (A) DHBV-infected PDHs were pulsed with BODIPY-TR-C_5 ceramide, fixed, and stained. DHBV (green) colocalized with all species of sphingolipid (red), which persists with brefeldin A treatment. Sphingolipid accumulation in bile ducts (small arrows) and in lipid vacuoles (large arrows) can be seen. (B) Infected polarized PDHs and DVP cells and nonpolarized DVNP cells show ubiquitous virus-lipid colocalization. FRET between virus and newly synthesized sphingolipid is marked in both polarized and nonpolarized cells. The pixel intensity along a line through the colocalized regions (orange) is shown in the graphs on the right. Blue, nuclei and TOTO-3. Bar, 5 μm.

been described, albeit in nonpolarized hepatocyte models (2, 12). The trafficking and export of hepatitis C virus and its core protein have been shown to depend on endosomal structures in HuH7 hepatocyte-derived cells (11). The export mechanisms for hepadnaviruses in physiologically relevant, polarized hepatocyte-derived cells have not been previously addressed. Here we have predominantly used DHBV to model HBV egress so that we could utilize a primary cell culture model where possible, especially to examine viral trafficking and infectivity.

We observed that cell polarity was necessary for the efficient export of DHBV from primary hepatocytes but was not required for viral replication, as evidenced by intracellular accumulation of infectious particles over time with diminishing cell polarity (Fig. 2). This was also seen in persistently infected human hepatocyte-derived cells, which maintained a steady rate of virus excretion for between 18 and 30 days in culture but demonstrated a more than 10,000-fold increase in intracellular virus during that time. Since the export pathways of adenovirus-transduced HBV and DHBV were the same (Fig. 3), it is likely that HBV export is also vectorial. Such dependence on cell polarity for virus export has significant implications for pathogenesis. Loss of cell polarity is characteristic of cholestatic liver disease, and recent studies have also demonstrated that hepatitis C virus (HCV) can directly down-modulate hepatocyte polarity (19). It is therefore likely that cholestasis and/or HCV coinfection could lead to increased intracellular retention of progeny HBV and viral antigen and, thus, increased pathological consequences.

The observed predominance of basolateral viral export is not surprising and is consistent with the default pathway for export of most substrates from hepatocytes, allowing direct export of infectious virus into the bloodstream. Indeed, we have previously shown that hepatitis A virus is almost exclusively exported from hepatocytes via the basolateral domain (26), even though its enteric transmission requires that HAV eventually be released into the bile and feces. Surprisingly, we observed apical release for a significant proportion of progeny DHBV

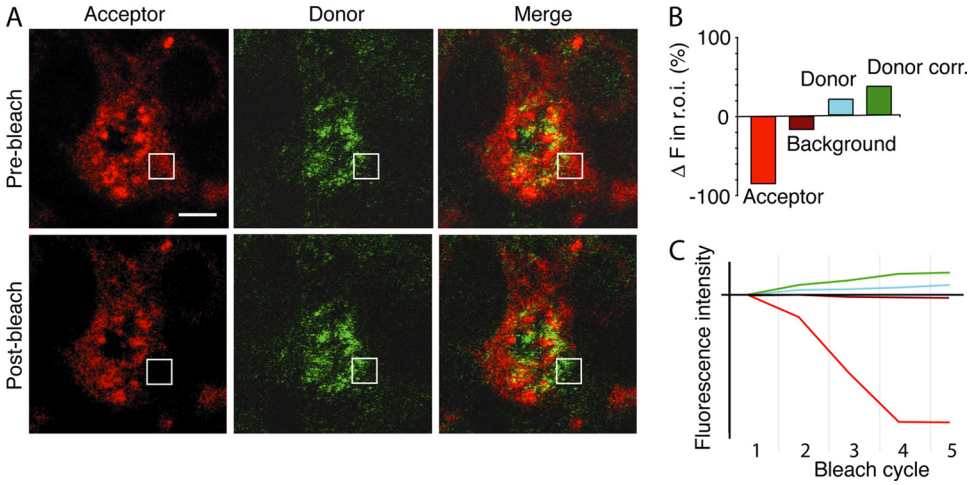

FIG. 7. FRET between sphingolipids and virus. (A) DHBV-infected PDHs were pulsed with BODIPY-TR-C_5 ceramide, fixed, and stained. The indicated square region of interest (r.o.i.) was photobleached over several cycles using a 543-nm laser line. Acceptor excitation-emission and donor excitation-emission images were then taken of the whole field. Donor fluorescence change in the r.o.i. was corrected for background photobleaching. (B) The acceptor fluorophore (red) was bleached, resulting in a quantifiable increase in the donor intensity (green) of over 15% above background in the r.o.i. (C) Progressive bleaching of the acceptor molecule over 5 cycles resulted in background bleaching (maroon), but in the r.o.i., the donor fluorophore intensity (blue) increased, resulting in a significant corrected fluorophore increase (donor correction [Donor corr.]; (green). The relative fluorescence intensity from the initial image with each bleach cycle is shown. Data shown are representative of at least 3 experiments with five regions bleached in each experiment. Bar, 5 μm.

from polarized N6 or DVP cells, which would be consistent with excretion of virus and antigen in bile. If this observation is also true of HBV, then it is interesting to note that the antigenicity of HBsAg has been shown to be preserved in the gastrointestinal tract (29). Although it appears to be unlikely that the infectious enveloped DHBV (or HBV) would survive exposure to bile salts, excretion of large amounts of viral antigen into bile and the enterohepatic circulation could have a significant role in promoting the development of immunological tolerance to HBV.

The transferrin trafficking pathway in hepatocytes is distinct from its pathway in other cells. In HepG2 cells, it has been elegantly shown to follow entry and bulk-flow traffic to the subapical compartment for sorting and recycling to the basolateral membrane (4, 40). In this study, although virus and transferrin colocalized in nonpolarized cells, DHBV did not appear to traffic with transferrin when the transportation of the two substrates was vectorially regulated, implying a differential transportation system, albeit one still dependent on cell polarity.

Sphingolipid trafficking in polarized hepatocytes is distinct from protein trafficking and is differentially regulated (7, 40), but it is also polarity dependent (7, 33). We saw a close physical association between sphingolipid and virus in hepatocytes, strongly implying a cotransportation mechanism. The nature of this virus-sphingolipid interaction remains conjecture. Enveloped viruses, being coated with lipoproteins, lend themselves to transport by sphingolipid rafts, as has been suggested for measles virus and HIV (17, 22, 24, 38). Additionally, the behavior of DHBV export from nonpolarized cells is consistent with the behavior of raft-dependent sorting, described to be similar in both polarized and nonpolarized hepatocytes (21).

We note that the antibody that we used to identify DHBV will not distinguish between subviral particles, which have identical envelope protein compositions (containing both S and L proteins). As such, we cannot exclude the possibility that the results of our colocalization studies reflect the fate of the excess of subviral particles rather than the minor proportion of intact virions; however, we believe that it is unlikely that these particles have different pathways. While it has been suggested that subviral particles in nonhepatocyte (MDCK) cells traffic by different routes to HBV particles (18), this would appear to be a function of the cells rather than the antigen because it is contrary to the mass export of both HBsAg and HBV virions into plasma from hepatocytes. In hepatocytes, synthesized DHBV and subviral particles have been shown to enter the same type of vesicular bodies after the endoplasmic reticulum (20), which reinforces the need to use hepatocyte-derived cells for the current studies.

It has been presumed that viruses, particularly noncytopathic viruses such as DHBV and HBV, hitch a ride on preexisting cellular mechanisms for transport within the cell and export from the cell. The determinants of this interaction, however, had not been studied. It is possible that similar sphingolipid-associated mechanisms may be utilized by other hepatotropic viruses, including hepatitis C virus. The findings of this study broaden our understanding of the mechanisms of pathogen export from hepatocytes.

ACKNOWLEDGMENTS

We thank Elizabeth Grgacic for assistance with primary duck hepatocytes.

This study was supported in part by a project grant and a senior research fellowship (to D.A.A.) from the National Health and Medical Research Council of Australia.

REFERENCES

1. **Anderson, D. A., E. V. Grgacic, C. A. Luscombe, X. Gu, and R. Dixon.** 1997. Quantification of infectious duck hepatitis B virus by radioimmunofocus assay. J. Med. Virol. **52:**354–361.

2. **Bardens, A., T. Doring, J. Stieler, and R. Prange.** 2011. Alix regulates egress of hepatitis B virus naked capsid particles in an ESCRT-independent manner. Cell. Microbiol. **13:**602–619.
3. **Blank, C. A., D. A. Anderson, M. Beard, and S. M. Lemon.** 2000. Infection of polarized cultures of human intestinal epithelial cells with hepatitis A virus: vectorial release of progeny virions through apical cellular membranes. J. Virol. **74:**6476–6484.
4. **Ciechanover, A., A. L. Schwartz, A. Dautry-Varsat, and H. F. Lodish.** 1983. Kinetics of internalization and recycling of transferrin and the transferrin receptor in a human hepatoma cell line. Effect of lysosomotropic agents. J. Biol. Chem. **258:**9681–9689.
5. **Fujiwara, T., K. Oda, S. Yokota, A. Takatsuki, and Y. Ikehara.** 1988. Brefeldin A causes disassembly of the Golgi complex and accumulation of secretory proteins in the endoplasmic reticulum. J. Biol. Chem. **263:**18545–18552.
6. **Funk, A., H. Hohenberg, M. Mhamdi, H. Will, and H. Sirma.** 2004. Spread of hepatitis B viruses in vitro requires extracellular progeny and may be codetermined by polarized egress. J. Virol. **78:**3977–3983.
7. **Hanada, K.** 2005. Sphingolipids in infectious diseases. Jpn. J. Infect. Dis. **58:**131–148.
8. **Hoekstra, D., O. Maier, J. M. van der Wouden, T. A. Slimane, and S. C. D. van IJzendoorn.** 2003. Membrane dynamics and cell polarity: the role of sphingolipids. J. Lipid Res. **44:**869–877.
9. **Jourdan, N., et al.** 1997. Rotavirus is released from the apical surface of cultured human intestinal cells through nonconventional vesicular transport that bypasses the Golgi apparatus. J. Virol. **71:**8268–8278.
10. **Kreitzer, G., et al.** 2003. Three-dimensional analysis of post-Golgi carrier exocytosis in epithelial cells. Nat. Cell Biol. **5:**126–136.
11. **Lai, C. K., K. S. Jeng, K. Machida, and M. M. Lai.** 2010. Hepatitis C virus egress and release depend on endosomal trafficking of core protein. J. Virol. **84:**11590–11598.
12. **Lambert, C., T. Doring, and R. Prange.** 2007. Hepatitis B virus maturation is sensitive to functional inhibition of ESCRT-III, Vps4, and gamma 2-adaptin. J. Virol. **81:**9050–9060.
13. **Lambert, C., and R. Prange.** 2007. Posttranslational N-glycosylation of the hepatitis B virus large envelope protein. Virol. J. **4:**45.
14. **Lentz, T. B., and D. D. Loeb.** 2010. Development of cell cultures that express hepatitis B virus to high levels and accumulate cccDNA. J. Virol. Methods **169:**52–60.
15. **Lewin, S., et al.** 2001. Analysis of hepatitis B viral load decline under potent therapy: complex decay profiles observed. Hepatology **34:**1012–1020.
16. **Maier, O., and D. Hoekstra.** 2003. Trans-Golgi network and subapical compartment of HepG2 cells display different properties in sorting and exiting of sphingolipids. J. Biol. Chem. **278:**164–173.
17. **Manie, S. N., S. Debreyne, S. Vincent, and D. Gerlier.** 2000. Measles virus structural components are enriched into lipid raft microdomains: a potential cellular location for virus assembly. J. Virol. **74:**305–311.
18. **Marzolo, M. P., P. Bull, and A. Gonzalez.** 1997. Apical sorting of hepatitis B surface antigen (HBsAg) is independent of N-glycosylation and glycosylphosphatidylinositol-anchored protein segregation. Proc. Natl. Acad. Sci. U. S. A. **94:**1834–1839.
19. **Mee, C. J., et al.** 2008. Effect of cell polarization on hepatitis C virus entry. J. Virol. **82:**461–470.
20. **Mhamdi, M., A. Funk, H. Hohenberg, H. Will, and H. Sirma.** 2007. Assembly and budding of a hepatitis B virus is mediated by a novel type of intracellular vesicles. Hepatology **46:**95–106.
21. **Nyasae, L. K., A. L. Hubbard, and P. L. Tuma.** 2003. Transcytotic efflux from early endosomes is dependent on cholesterol and glycosphingolipids in polarized hepatic cells. Mol. Biol. Cell **14:**2689–2705.
22. **Phalen, T., and M. Kielian.** 1991. Cholesterol is required for infection by Semliki Forest virus. J. Cell Biol. **112:**615–623.
23. **Saucan, L., and G. E. Palade.** 1994. Membrane and secretory proteins are transported from the Golgi complex to the sinusoidal plasmalemma of hepatocytes by distinct vesicular carriers. J. Cell Biol. **125:**733–741.
24. **Scheiffele, P., A. Rietveld, T. Wilk, and K. Simons.** 1999. Influenza viruses select ordered lipid domains during budding from the plasma membrane. J. Biol. Chem. **274:**2038–2044.
25. **Slimane, T. A., G. Trugnan, S. C. D. Van IJzendoorn, and D. Hoekstra.** 2003. Raft-mediated trafficking of apical resident proteins occurs in both direct and transcytotic pathways in polarized hepatic cells: role of distinct lipid microdomains. Mol. Biol. Cell **14:**611–624.
26. **Snooks, M. J., et al.** 2008. Vectorial entry and release of hepatitis A virus in polarized human hepatocytes. J. Virol. **82:**8733–8742.
27. **Sprinzl, M., H. Oberwinkler, H. Schaller, and U. Protzer.** 2001. Transfer of hepatitis B virus genome by adenovirus vectors into cultured cells and mice: crossing the species barrier. J. Virol. **75:**5108–5118.
28. **Stoorvogel, W., H. J. Geuze, J. M. Griffith, and G. J. Strous.** 1988. The pathways of endocytosed transferrin and secretory protein are connected in the trans-Golgi reticulum. J. Cell Biol. **106:**1821–1829.
29. **Thanavala, Y., et al.** 2005. Immunogenicity in humans of an edible vaccine for hepatitis B. Proc. Natl. Acad. Sci. U. S. A. **102:**3378–3382.
30. **Tugizov, S. M., J. W. Berline, and J. M. Palefsky.** 2003. Epstein-Barr virus infection of polarized tongue and nasopharyngeal epithelial cells. Nat. Med. **9:**307–314.
31. **Uchida, T., K. Suzuki, Y. Okuda, and T. Shikata.** 1988. In vitro transmission of duck hepatitis B virus to primary duck hepatocyte cultures. Hepatology **8:**760–765.
32. **van IJzendoorn, S. C., and D. Hoekstra.** 1998. (Glyco)sphingolipids are sorted in sub-apical compartments in HepG2 cells: a role for non-Golgi-related intracellular sites in the polarized distribution of (glyco)sphingolipids. J. Cell Biol. **142:**683–696.
33. **van IJzendoorn, S. C., and D. Hoekstra.** 2000. Polarized sphingolipid transport from the subapical compartment changes during cell polarity development. Mol. Biol. Cell **11:**1093–1101.
34. **van IJzendoorn, S. C., M. M. Zegers, J. W. Kok, and D. Hoekstra.** 1997. Segregation of glucosylceramide and sphingomyelin occurs in the apical to basolateral transcytotic route in HepG2 cells. J. Cell Biol. **137:**347–357.
35. **Wagner, M., A. K. Rajasekaran, D. K. Hanzel, S. Mayor, and E. Rodriguez-Boulan.** 1994. Brefeldin A causes structural and functional alterations of the trans-Golgi network of MDCK cells. J. Cell Sci. **107**(Pt 4)**:**933–943.
36. **Wakabayashi, Y., P. Dutt, J. Lippincott-Schwartz, and I. M. Arias.** 2005. Rab11a and myosin Vb are required for bile canalicular formation in WIF-B9 cells. Proc. Natl. Acad. Sci. U. S. A. **102:**15087–15092.
37. **Wang, C.-Y. J., J. J. Giambrone, and B. F. Smith.** 2002. Development of viral disinfectant assays for duck hepatitis B virus using cell culture/PCR. J. Virol. Methods **106:**39–50.
38. **Wang, J. K., E. Kiyokawa, E. Verdin, and D. Trono.** 2000. The Nef protein of HIV-1 associates with rafts and primes T cells for activation. Proc. Natl. Acad. Sci. U. S. A. **97:**394–399.
39. **Wang, L., and J. L. Boyer.** 2004. The maintenance and generation of membrane polarity in hepatocytes. Hepatology **39:**892–899.
40. **Wustner, D.** 2006. Quantification of polarized trafficking of transferrin and comparison with bulk membrane transport in hepatic cells. Biochem. J. **400:**267–280.
41. **Wustner, D., S. Mukherjee, F. R. Maxfield, P. Muller, and A. Herrmann.** 2001. Vesicular and nonvesicular transport of phosphatidylcholine in polarized HepG2 cells. Traffic **2:**277–296.
42. **Zegers, M. M., K. J. Zaal, S. C. van IJzendoorn, K. Klappe, and D. Hoekstra.** 1998. Actin filaments and microtubules are involved in different membrane traffic pathways that transport sphingolipids to the apical surface of polarized HepG2 cells. Mol. Biol. Cell **9:**1939–1949.